Pathologic Scar Formation

Morphologic and Biochemical Correlates

T. R. Knapp, MD, J. R. Daniels, MD, and E. N. Kaplan, MD

Morphologic and biochemical analyses were performed to compare normal skin and mature scars to hypertrophic scar and keloid. Correlation of morphologic findings with biochemical profiles of the skin and scar samples proved feasible and enlightening. Scanning electron microscopy (SEM) was used to characterize the architectural arrangement of collagen fibers in skin and scars. Cultured fibroblasts from each specimen were also examined with the SEM. A biochemical profile of each tissue specimen was constructed, characterizing the collagen component of the specimen by sequential molecular sieve and ion exchange chromatography to determine a) the degree of intermolecular crosslinking, b) amino acid analysis, and c) levels of lysyl oxidase activity. Results indicate that collagen fibers and fiber bundles display a decreasing level of organization as the clinical degree of scar abnormality increases, and this structural gradient correlates with the gradient of intermolecular crosslinking in the same tissue—normal skin and mature scar being highly crosslinked, hypertrophic and keloid successively less so. Surprisingly, the level of the crosslinking enzyme lysyl oxidase is normal or elevated in hypertrophic scar and keloid despite the relative lack of crosslinking. Amino acid content was uniform for all specimens. Scanning electron microscopy examination of cultured fibroblasts from the tissue specimens demonstrated three phenotypically distinctive fibroblasts whose numerical and volumetric proportions correlated with the tissue of origin. (Am J Pathol 86:47–70, 1977)

CURRENTLY RECOGNIZED CLINICAL AND LABORATORY METHODS only partially succeed in characterizing hypertrophic scar and keloid and do not fully explain their behavior. Previous investigations have explored in isolated fashion the morphology of fibroblasts cultured from keloid and hypertrophic scar; the microarchitecture of scar; various biochemical parameters of cultured scar tissue; or selected chemical components of the scars themselves.[1] Based on these studies, it is felt that persistent scar hypertrophy and keloid formation represent apparent defects in the metabolic control of scar formation which lead to a pathologic accumulation of fibrous connective tissue—and most particularly the collagen component.

We felt that it would be profitable to explore systematically and in analytical fashion both morphologic and biochemical parameters in abnormal and normal scar specimens. This study was designed to examine morphologic, cellular, and biochemical aspects of scar formation, com-

From the Department of Surgery, Division of Plastic and Reconstructive Surgery, and the Department of Medicine, Stanford University School of Medicine, Stanford, California.

Dr. Knapp is the recipient of a fellowship from the Bank of America–Giannini Foundation.

Accepted for publication August 10, 1976.

Address reprint requests to Dr. Terry R. Knapp, Department of Surgery, Division of Plastic and Reconstructive Surgery, Stanford University School of Medicine, Stanford, CA 94305.

paring skin and mature scar to putative hypertrophic scar and keloid. The morphology of the collagen weave and tissue culture–derived fibroblasts of representative tissue specimens was examined with the scanning electron microscope. Structural relationships of collagen fibers and bundles were observed; fibroblasts were sorted, classified according to appearance and average size, and then correlated with tissue of origin. A biochemical profile for each tissue specimen was constructed characterizing the collagen component by its degree of crosslinking, α-chain and amino acid composition, and the lysyl oxidase activity in the tissue specimens.

Background Information

Collagen is the principle extracellular protein synthesized during active fibrosis and is the dominant material in mature scar.[2] The maturation of collagen involves the progressive loss of solubility by extensive crosslink formation.[3-7]

The collagen molecule is an asymmetric rigid rod with dimensions of 15 $\times$ 3000 Å and a molecular weight of approximately 300,000. Each molecule consists of three polypeptide chains—designated α-chains—each containing approximately 1000 amino acid residues. Throughout the course of most of the molecule, polypeptide strands are arrayed in the unique collagen helix pattern. In the helical portion of each polypeptide chain every third residue is glycine. These glycyl residues occupy the axial plane of the helix.

Prior to secretion of the molecule from the cell, several biochemical events occur: the collagen α-chains are thought to be aligned in the triple helix in appropriate registration by large amino terminal extensions (about 20,000 daltons) which are then cleaved by procollagen peptidase; many prolyl and lysyl residues are enzymatically hydroxylated by prolyl and lysyl hydroxylases—the degree of hydroxylation at each site varies depending in part on species and tissue specificity; and glycosylation takes place by the sequential addition of galactose and glucose to specific hydroxylysines.[8]

The completed collagen molecules are secreted by the cell into the extracellular space as single tropocollagen molecules. Collagen molecules form fibrils by precipitating in a linear, quarter-stagger array. Fibril formation proceeds spontaneously in the extracellular space under physiologic conditions.

Crosslink formation is important in fibril stabilization. Intramolecular crosslinks exist within each molecule between polypeptide chains in the nonhelical amino terminal portion. Intermolecular crosslinks within the fibril are much more extensive and link many single molecules into a large polymer.

Crosslinking proceeds when the ϵ-amino group of specific lysyl residues, predominantly those in the amino terminal region, undergo enzymatic oxidative deamination—mediated by lysyl oxidase—to the α-amino adipic δ-semialdehyde.[9] Crosslinks are formed when oxidized residues on adjacent chains undergo aldol condensation reactions or when Schiff base formation takes place between an oxidized lysyl or hydroxylysyl residue and one which has not been modified—or possibly with another amine. These Schiff bases become stabilized by subsequent reduction. The efficiency of lysyl oxidase activity may be regulated by the type of fibril on which it acts—the rate of crosslinking being dependent on the rate and integrity of collagen fibril formation.[10]

Skin and bone collagens are composed primarily of two types of α-chain: $\alpha 1(I)$ and $\alpha 2$.[7] The designated formula for the molecular α-chain composition of collagen of this type is $[\alpha 1(I)_2 \alpha 2]$. This is known as Type I collagen. Cartilage collagen is unique, consisting of three identical α-chains of different sequence from the Type I alpha chains.[11,12] Cartilage collagen has the formulation $[\alpha 1(II)]_3$ and is known as Type II collagen. A cysteine-containing interstitial collagen has been identified in human fetal and newborn dermis, the media of large blood vessels, and uterine fibromata.[13] This Type III collagen is formulated $[\alpha 1(III)]_3$. Basement membrane collagen, designated Type IV, is a distinctive species with a high molecular weight which contains cysteine.[14,15]

Collagen degradation as well as synthesis is an important process in developing the final connective tissue result of growth or repair. Mammalian collagenases are a group of specific collagenolytic enzymes capable of cleaving the native collagen molecule in a single region three-quarters from the amino terminus.[16] Collagenase may often be harvested from cultures of collagen-rich tissues, and its level may often correlate with active resorption.[17-19]

Materials and Methods

Normal skin samples were taken from healthy individuals undergoing elective surgery. Scar specimens were obtained by surgical excision performed as part of the treatment of the scar. All scars utilized in this study were the result of wounds sustained as least 1 year prior to treatment. The designation of hypertrophic scar or keloid was assigned to specimens based on clinical judgment and recognized criteria.

Morphology

Gross Tissue Preparation

Eleven normal skin specimens (face or torso), twelve mature scars, seven hypertrophic scars, and eleven keloids were excised and portions of the specimens glued epithelial-side-

down to blocks of Silastic (Dow Corning Corp.) to allow fixation under physiologic tension. The tissues were fixed in 4% formalin at 4 C for 1 week and then were sectioned on the freezing stage of a sliding microtome to a thickness of 100 to 200 μ. Sections were taken both parallel and perpendicular to the epithelial surface.

The specimens were then exposed to crude bacterial α-amylase,[20] washed in phosphate buffer, and carried through graded ethanol and amyl-acetate solutions to displace tissue water. To eliminate surface artifacts, the tissues were dried from 100% amyl-acetate using the critical point drying technique with liquid CO_2 medium.[21]

The dried specimens were mounted on aluminum studs with colloidal silver paint and coated sequentially with vaporized carbon and gold-palladium 60–40 to a coating depth of approximately 150 Å. The specimens were then viewed under an AMR (Applied Materials Research, Inc.) model 900 scanning electron microscope in the emissive mode at accelerating voltages up to 20 kV.

Routine hematoxylin and eosin–stained sections cut parallel and perpendicular to the epithelial surface were obtained on each specimen.

Fibroblast Preparation

Primary explants of dermal minces, dissected free of epithelium, were placed on coverslips in Eagle's minimal essential medium, pH 7.0, enriched with 10% calf serum, pyruvate, and ascorbic acid at 37 C in a 5% CO_2 atmosphere. When the cells were near confluency on the coverslip in Phase I fibroblast growth, the tissue explants were removed, and the coverslips immersed in 3% gluteraldehyde for 72 hours. The slips containing the fixed cells were gently washed in phosphate buffer, then prepared with critical point drying and mounted an aluminum studs.

Fibroblast Sizing

Cell outgrowths from several representative specimens were trypsinized free of their coverslips and passed into petri dishes. Upon reaching confluence from this first passage (Phase II, passage 1),[22] the cells were exposed to 0.3% trypsin at room temperature for 5 to 10 minutes, washed twice with buffered saline, and dispersed in buffered saline, pH 7.0, with gentle mechanical stirring to achieve a uniform single cell suspension.

A cell volume analyzer [23] was calibrated with chicken red blood cells (7-μ diameter) and paper mulberry pollen (12- to 14-μ diameter). Population distribution curves were then obtained for the various cell samples.

Biochemistry

Preparation of Starting Material

Portions of many of the tissue specimens which contributed information regarding collagen and cellular morphology were lyophilized, powdered in a Wiley mill, and solubilized with controlled enzymatic hydrolysis. Hydrolysis was accomplished with pepsin at temperatures low enough to confine hydrolysis to the nonhelical amino terminal and perhaps carboxyterminal peptide segments, preserving 95% of the molecule initially present. In this way, sequences adjacent to the intramolecular crosslinks and those intermolecular crosslinks which involve these regions are interrupted, resulting in effective solubilization of many connective tissue collagens.[24]

Denaturation of pepsin-prepared collagens results in the release of α-chains as well as a series of higher molecular weight aggregates (*vide infra*). It is a reasonable inference that these higher molecular weight aggregates are derived from the intermolecular crosslinks involving the pepsin-resistant peptides and that the degree of intermolecular crosslinking initially present correlates well with the extent of residual aggregation.

In this study, the tissue powders were exposed to pepsin (Sigma Chemical Co.) at a

concentration of 1:20 (w/w) of pepsin to tissue powder in 0.5 N acetic acid for 1 week at 11 C. An aliquot of this suspension was assayed for total hydroxyproline content. The insoluble residue was removed by centrifugation (30,000*g* for 30 minutes) and the supernate brought to neutral pH with NaOH, adjusting the [Na^+] to 1 M with NaCl. The resulting percipitate, containing denatured pepsin, was removed by centrifugation. The collagen in solution was then precipitated by the addition of NaCl to 3 M Na^+ and centrifugation (30,000*g* for 30 minutes). The collagen precipitate was redissolved in 0.5 N acetic acid and reprecipitated from the acid by addition of NaCl (5% w/v). The purified collagen precipitate was retrieved by centrifugation (30,000*g* for 30 minutes) and redissolved in 0.5 N acetic acid, dialyzed against 0.001 N acetic acid, and lyophilized. This collagen preparation was the starting material (SM) for subsequent analyses. Recovery of collagen was calculated by measuring hydroxyproline in SM as a fraction of total hydroxyproline initially present.

Sequential Chromatography

Samples of the purified SM were dissolved in water and adjusted to 1 M $CaCl_2$, 0.01 M Tris Cl, pH 7, denatured by addition of solid urea to 8 M, and applied to agarose molecular sieve columns to separate the components of the SM into α, β (two covalently bound α-chains), γ (three α-chains), and higher aggregate fractions. To determine the presence of Type III collagen in SM, the agarose molecular sieve column patterns from representative SMs were compared with and without prior reduction and alkylation.

The α-chain fractions retrieved from the molecular sieve columns were dialyzed against a 0.06 sodium acetate, pH 4.8, starting buffer and applied to a carboxymethyl cellulose (CMC) cation exchange column at 45 C with an elution gradient of 0 to 0.1 N NaCl for separation of the α1 and α2 chains.

Amino Acid Analysis

Starting material and α1 and α2 chains were hydrolyzed for amino acid analysis on a Beckman model 120C amino acid analyzer using the single column, multiple buffer technique as described.[14]

Lysyl Oxidase Activity

Representative fractions of gross tissue powders from each type of specimen were kindly analyzed by Dr. Robert Siegel for lysyl oxidase activity according to his methods.[9,10]

Results

Morphology

Tissue

Normal Skin and Mature Scar. Low-power views of the collagen weave of normal skin cut parallel to the epithelial surface demonstrate a vast network of distinct collagen bundles, the majority of which run parallel to the epithelial surface (Figure 1A). Perpendicular sections confirm this arrangement. The bundles of collagen fibers are discrete in their interrelationships, but appear to be randomly connected with other collagen bundles by fine fibrilar strands of collagen or perhaps elastin. The individual bundles are on the order of 8 to 10 μ in diameter.

High-power magnification of individual collagen bundles demonstrates

that the fibers lie in parallel array and are closely packed (Figure 1B).

The interrelationship of collagen bundles appears less structured in mature scar than in skin. Individual bundle morphology, however, is indistinguishable from that of normal skin.

Hypertrophic Scar. The collagen weave of hypertrophic scar is decisively different from that of normal skin or mature scar (Figure 2A). Collagen bundles are flatter and less clearly demarcated. Bundle interrelationships appear less structured, though the majority of bundles still appear to run parallel to the epithelial surface.

At higher magnification the fibers comprising the collagen bundles appear loosely arrayed in a wavy pattern and often appear somewhat fragmented and shortened (Figure 2B).

Keloid. Keloid collagen ultrastructure demonstrates even less apparent organization than does hypertrophic scar (Figure 3A). Discrete bundle formation is virtually absent; collagen fibers lie in haphazardly connected loose sheets which appear oriented randomly with respect to the epithelial surface.

Higher magnification further demonstrates the random nature of fiber orientation, inconsistency in fiber length, and failure of bundle formation (Figure 3B).

Fibroblast

The cellular outgrowths from the various tissue samples resulted in pleomorphic populations of fibroblasts. However, several phenotypically different fibroblast variants could be distinguished, and the relative distribution of these variants differed systematically with the tissue of origin.

Normal skin, mature scar, and hypertrophic scar fibroblasts were predominantly of two types: a small spindle-shaped cell (designated the *S cell*) and a larger, flatter more ameboid-appearing cell (designated the *A cell*).

High-power views of the S-cell type revealed a distinctly bipolar fibroblast with a rough, lobulated cell surface. Fine strands of material emanated from the base of such cells in a radial direction (Figure 4).

A cells, which seem to predominate in the keloid-derived fibroblast populations, were rather flat, quite large, and possessed a smoother surface. Pseudopod-like extensions were a feature of this cell.

Hypertrophic scar-derived fibroblasts were composed of many of both the A and S cells, grouped randomly one among the other (Figure 5).

There were very few S cells in outgrowths from the keloid specimens. A third type of cell, designated the *K cell*, often characterized keloid outgrowths. The K fibroblast was intermediate in size and appeared nearly

unipolar with a blunted fore and long tailing cytoplasmic process (Figure 6). Table 1 represents an estimated frequency of occurrence of cell type according to tissue of origin. It seems that keloid is composed primarily of larger cell types and that a substantial number of smaller S cells exists in the other tissues studied.

Fibroblast Sizing

Table 2 represents the analysis of cell sizes of representative cell outgrowths from each of the tissue types. The data suggest that the average cell size of most keloid cell populations measured had mean cell sizes significantly larger than the fibroblast populations from the other tissue sources ($P < 0.001$).

Biochemistry

Recovery of Collagen From Tissue Specimens

The estimate of collagen recovered, measured as percent hydroxyproline recovered in SM relative to the levels of hydroxyproline in the whole tissue, was uniformly high (80 to 90% recovery for all specimens).

Chromatography

The molecular sieve chromatographic pattern derived from pepsin solubilized normal skin collagen following denaturation is shown in Text-figure 1. Peaks are identified corresponding to α, β, and γ chains and an excluded peak in a position consistent both with tetramers and with higher aggregates is denoted I. Persistent aggregation after pepsin solubilization is interpreted to be a function of intermolecular crosslinks involving pepsin-resistant sequences.

Text-figure 2 is a similarly derived pattern typical of three of the four keloid specimens examined. The differences are dramatic, with predominance of the α-chain fraction and corresponding diminution of the higher aggregates.

Subsequent chromatography of the agarose isolated α-chains on col-

Table 1—Frequency of Occurrence of Cell Types

Specimen	No. of cells counted	S	A	K
Normal skin	55	70%	30%	0
Mature scar	105	50%	40%	10%
Hypertrophic scar	98	60%	35%	5%
Keloid	58	10%	60%	30%

Table 2—Fibroblast Population Distribution

Specimen	Cells sized $\times 10^3$	Mean cell diameter (μ)	Calculated mean cell volume (cu μ)
3A Normal skin	23.3	13.9 ± 1.8	1396
2A Normal skin	28.8	15.7 ± 2.5	2012
3B Mature scar	26.3	15.9 ± 2.2	2090
2C Hypertrophic scar	26.7	15.4 ± 2.2	1899
3D Keloid	24.7	15.7 ± 2.3	2012
2D Keloid	32.0	16.4 ± 2.6	2294
1D Keloid	35.3	17.1 ± 2.4	2600

umns of CMC have provided a second intriguing observation. The patterns observed for α-chains of normal skin and keloid are shown in Text-figure 3. The relative peak area of $\alpha 1 : \alpha 2$ for skin is 6.4, and for keloid is less than 3.

Table 3 summarizes the chromatography data for the specimens analyzed. The relative α-chain content of each specimen SM results in an ordered gradient in α-chain content from 46% for normal skin to 91% for keloid—with normal skin and scar having proportionately higher contents of heavily crosslinked fractions (β, γ, and higher aggregates), and hypertrophic scar and keloid successively less. A single anomalous specimen (specimen 9D) represents a clinically older earlobe keloid which was soft and had been quiescent for a number of months prior to resection.

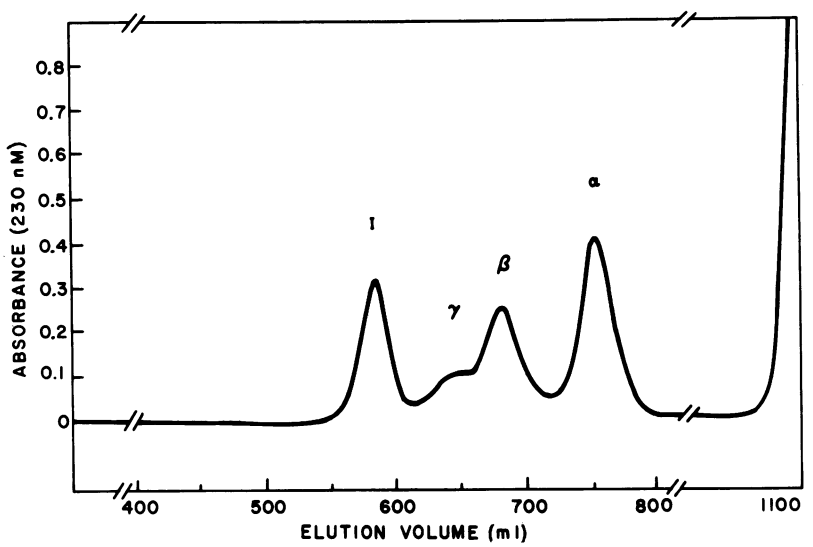

TEXT-FIGURE 1—Molecular sieve pattern of pepsin-solubilized, denaturated normal skin collagen. The α-chain component is equaled by the numbers of higher aggregates present.

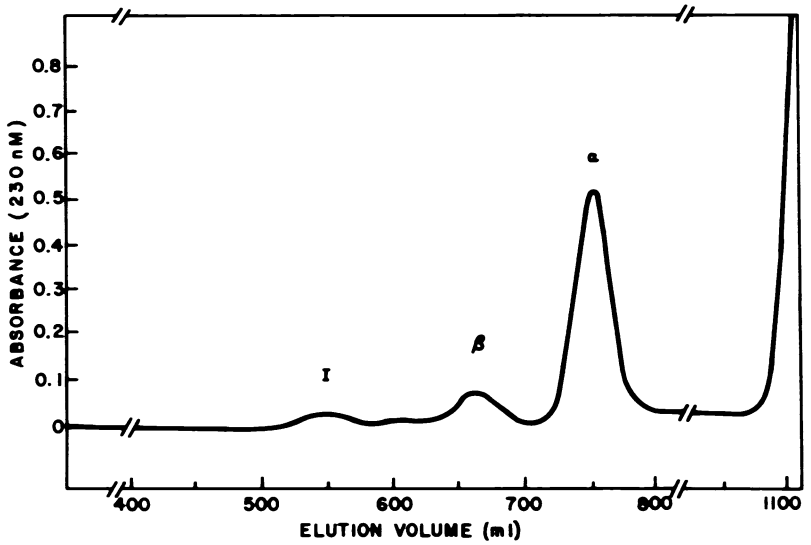

TEXT-FIGURE 2—Molecular sieve pattern of pepsin solubilized, denatured keloid collagen. The α-chains are the dominant component of the keloid collagen preparation.

Examining the ratio of $\alpha 1$ to $\alpha 2$ from each specimen, one can rank with good correspondence this ratio inversely with the proportion of collagen separating as α-chains on agarose. Piez [7] has shown in dogfish collagen that, with respect to dimers, there is more $\beta_{1\text{-}2}$ relative to $\beta_{1\text{-}1}$ than would have been expected on the basis of the 2:1 ratio of $\alpha 1$ to $\alpha 2$. These findings, together with the data presented here, suggest a special role for the $\alpha 1$–$\alpha 2$ association in the formation of crosslinks. Alternatively, the apparent selective incorporation of $\alpha 2$ into crosslinks may reflect relative resistance to pepsin digestion of the amino terminal region of the $\alpha 2$ chain.

It was anticipated that alteration of peak height on agarose chromatography by prior reduction and alkylation of SM would suggest the presence of disulfide crosslinks as have been found in cysteine-containing collagens.[13] No such alteration of relative peak amplitude was observed on representative SM samples so treated.

Amino Acid Anlyses

Amino acid analyses of SM, $\alpha 1$, and $\alpha 2$ chains from normal skin and all scar specimens yielded uniform and appropriate amounts of amino acid residues. Cysteine—determined as a carboxymethyl derivative (and present in Type III collagen)—has not been detected on the amino acid analysis of any of the specimens.

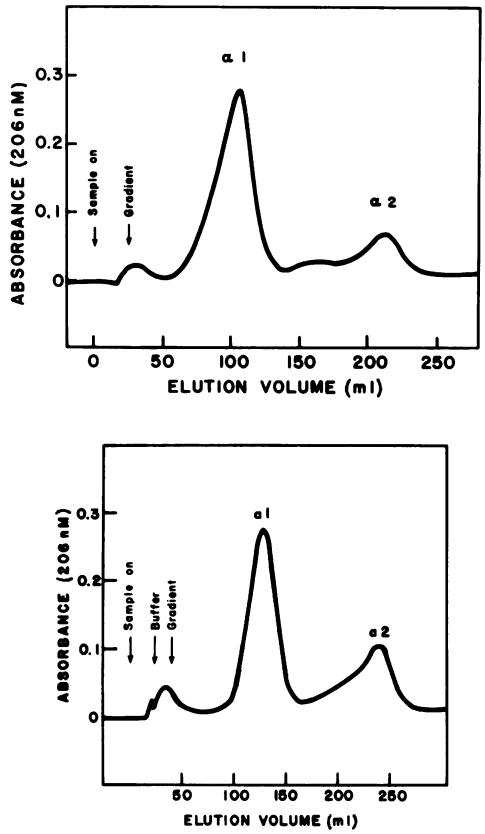

TEXT-FIGURE 3—Cation exchange column chromatographs of normal skin (**top**) and keloid α-chain components retrieved from molecular sieve chromatography (**bottom**). $\alpha 1 : \alpha 2$ ratio obtained by integrating peak areas is 6.4 for normal skin but less than 3 for keloid.

Lysyl Oxidase Activity

Lysyl oxidase activity in various normal skin and scar specimens was measured as counts per minute of ^3H released from a collagen substrate labeled with tritium (^3H) on the C_6 carbon—the site of the -OH group oxidized by the enzyme. Table 4 summarizes this data.

Hypertrophic scar and keloid demonstrate levels of lysyl oxidase activity which are equivalent to or greater than those of normal skin and mature scar. Specimen 12A represents normal skin taken from a site adjacent to the 12D keloid. The keloid exhibited nearly three times the lysyl oxidase activity observed in the normal skin from the same patient.

Discussion

Recent work suggests a sustained accelerated rate of turnover in abnormal scars.[1,25,26] The activity of prolylhydroxylase, an enzyme associated

Table 3—Summary of Chromatography Data

Sample	Type	Age of specimen	Age of patient	Percent α on Ag	$\alpha 1 : \alpha 2$ CMC
10A	Normal skin	20 yrs	20 yrs	45.5%	6.4
9A	Normal skin	23 yrs	23 yrs	49.7%	—
12B	Normal scar	12 mons	3 yrs	58.8%	3.8
13B	Normal scar	18 mons	6 yrs	59.9%	—
9D	Keloid?	18 mons	15 yrs	61.7%	4.6
4C	Hyper scar	24+ mons	53 yrs	64.21%	4.1
6C	Hyper scar	12+ mons	10 yrs	74.1%	3.96
11D	Keloid	42 mons	30 yrs	81%	2.97
7D	Keloid	24 mons	58 yrs	83%	—
8D	Keloid	18 mons	9 yrs	91%	2.32

with collagen synthesis, is elevated, and there is some evidence suggesting a concurrent elevation of collagenolytic activity.

The biosynthesis of collagen and its assembly into fibers and bundles in the repair of wounded skin involves a complex series of biochemical events. In pathologic scar formation, observed alterations in morphology of the end product may be a reflection of an alteration of one or more of these events.

Figure 7 depicts a schematic model for discussion of the potential sites of biochemical control of connective tissue metabolism and structure. These sites of control can then be related to the observed abnormal morphology and biochemistry of keloid and hypertrophic scar that have been demonstrated in this study.

Gene Product and Intracellular Events (Figure 7-1)

Collagen Synthesis

The production of a faulty collagen as an altered gene product does not appear to account for the changes in structure we have described. We studied the collagen of normal skin and various scars by its chromatographic behavior and amino acid content. The methods used failed to demonstrate other than Type I collagen in normal skin, mature scar, hypertrophic scar, or keloid.

Hydroxylation

Amino acid analysis of various collagen fractions from each tissue type revealed uniform degrees of hydroxylation of prolyl and lysyl residues. These data indicate that hydroxylation of the α-chains as an intracellular event is not responsible for the subsequent abnormalities in inter-

Table 4—Lysyl Oxidase Activity in Skin and Scars

Specimen		^{3}H-release (counts/min/mg tissue ± 10%)
15A	Normal skin	5.3
19A	Normal skin	9.6
16A	Normal skin	17.3
$12A_d$	Normal skin*	16.1
12B	Mature scar	9.5
10B	Mature scar	23.4
11B	Mature scar	31.3
5C	Hypertrophic scar	13.2
9C	Hypertrophic scar	26.6
7C	Hypertrophic scar	49.6
12D	Keloid*	40.0
11D	Keloid	16.8

* Same patient.

molecular crosslinking and the architecture seen in hypertrophic scar and keloid.

Glycosylation

The glycosylation of collagen from a variety of tissues and species has been studied in detail.[27-29] There seems to be a consistent relationship between fiber size and the degree of glycosylation of the collagen involved. A high carbohydrate content is usually found when larger diameter fibers are present. We have not yet measured the glycosylation of hypertrophic scar and keloid collagen. However, consideration of the role that such an alteration may play in fibril formation and subsequent crosslinking is essential (*vide infra*).

Fibril Formation (Figure 7-2)

It has been suggested that fibril formation may be affected by the degree of glycosylation of tropocollagen in one of two ways—either covalent bonding to carbohydrate of hydroxylysyl residues may alter the number of hydroxylysyl residues available for crosslink formation and ultimate fibril stabilization or an increase in degree of collagen peptide glycosylation may, by steric hindrance, prevent normal fibril formation.[14,27-29]

Fibril Formation and Lysyl Oxidase Activity (Figure 7-3)

The aforementioned data are important in light of recent work by Siegel [10] concerning lysyl oxidase–mediated crosslinking and its relationship to collagen fibril formation. Working with highly purified prepara-

tions of lysyl oxidase, he has shown that when collagen is used as an *in vitro* substrate, lysyl oxidase activity proceeds rapidly after an initial lag phase. When spontaneous fibril formation is inhibited, lysyl oxidase demonstrates little activity. Siegel's data strongly suggest that lysyl oxidase–mediated crosslink formation *in vitro* procceds after the onset of fibril formation and that the rate and perhaps structural characteristics of fibril formation may modulate the formation of *in vivo* crosslinks.

Chromatographic data from our study demonstrate an increase in persistence of higher aggregates in normal skin and scar following pepsin digestion as compared with hypertrophic scar and keloid. These aggregates presumably represent intermolecular crosslinks not susceptible to pepsin digestion. One possible explanation for the lesser degree of intermolecular crosslinking observed in hypertrophic scar and keloid is inefficient lysyl oxidase activity secondary to faulty fibril formation.

Lysyl oxidase activity in keloid and hypertrophic scar tissues appears to be the equivalent of—or even greater than—the levels of lysyl oxidase activity in normal skin and mature scar. Therefore, no extractable direct inhibitor of lysyl oxidase activity is present.

Other than faulty fibril formation, an alternate explanation of lysyl oxidase inhibition—preventing intermolecular crosslink formation—would be the presence of an unknown substance in the abnormal scars which interferes with crosslink formation after the lysyl-derived aldehyde is formed. For example, cystein, penicillamine, and other analogs act in this manner.[30]

Glycosaminoglycans and the Formation of Fibers and Fiber Bundles (Figure 7-4)

There is considerable evidence that the control of the biosynthesis of both collagen and the ground substance glycosaminoglycans (GAGs or mucopolysaccharides) are interdependent.[31] For example, it has been observed that in tissues having the largest content of GAG there is correspondingly less organization in collagen structure.[32-34]

Kisher and Shetlar[35] have studied the interrelationship of GAGs and the collagen of hypertrophic scar. They examined collagen morphology of hypertrophic scar both with transmission electron microscopy (TEM) and scanning electron microscopy (SEM) and found a distinct lack of discrete fiber and bundle morphology much as we have described. The morphologic picture was correlated with a marked increase in chondroitin-4-sulfate in hypertrophic scar determined by cellulose acetate electrophoresis on papain-digested specimens. Levels of hyaluronic acid and dermatan sulfate, the other commonly occurring skin glycosaminoglycans, were normal.

These authors also postulated that the increase in ground substance was responsible for interference with collagen fibril aggregation. Furthermore, they suggest that the stimulus for new collagen production may reside in an overabundance of chondroitin-4-sulfate.

Collagenolytic Remodeling of Fibrous Tissue (Figure 7-5)

It is known that the site of collagenase production by normal human skin is in the papillary layer of the dermis and that in open wounds both epithelium and mesenchymal tissues actively produce collagenase.[36,37] Cohen [1] has reported, without delineating the method used, a significant increase in collagenolytic activity in normal scar as well as hypertrophic scar and keloid beyond that found in normal skin. Keloid was said to demonstrate twice the collagenolytic activity of hypertrophic scar. At present, there is no evidence to suggest that such collagenase activity in scars is other than a compensatory response to an increase in fibrous tissue deposition. It is interesting to speculate, however, that increased collagenolytic activity in hypertrophic scar and keloid may be a response to the abnormal end architecture of the collagen fibers and bundles in these tissues.

Feedback-Controls (Figure 7-6)

In scar formation and maturation, as in any dynamic biologic system, feedback controls must be operative. It is conceivable that faulty end-product formation—such as the abnormally organized collagen bundles we have demonstrated in hypertrophic scar and keloid—stimulates compensatory collagenolytic activity. It is not known whether resulting collagen degradation products or, somehow, other elements associated with the abnormally organized connective tissue either fail to repress collagen production, actively stimulate it, or both.

Rokosova-Cmuchalova and Bentley [38] have shown that collagen synthesis may be specifically interdependent with chondroitin sulfate synthesis. The observation of an increase in chondroitin-4-sulfate content in hypertrophic scar lends credence to the notion that the GAG component of connective tissue may directly affect the final form of the fibrous matrix and may possibly directly or indirectly influence the degree of production of the collagen component of the matrix.

Role of the Fibroblast (Figure 7-7)

It is not known whether the same fibroblasts which produce the GAG component of connective tissue also actively produce the collagenous

component. Collagen, GAGs, and collagenase are all fibroblast products. It is conceivable that fibroblasts selectively producing one of these complexes might be morphologically distinct from fibroblasts producing a different moiety. Our identification of morphologic variants of fibroblasts in skin and abnormal scars with numerical ratio of such variance dependent on tissue origin provides impetus to approach these cellular parameters regulating connective tissue metabolism via mass cultures, serial subcultures, and cloned passages of distinctive morphologic phenotypes.

Summary

We have demonstrated that collagen fibers and fiber bundles display a decreasing level of organization as the clinical degree of scar abnormality increases and that this structural gradient correlates with the gradient of intermolecular crosslinking in the same tissues—normal skin, mature scar, hypertrophic scar, and keloid being successively less crosslinked. Surprisingly, the enzyme which initiates intermolecular crosslinks—lysyl oxidase—is normal or elevated in hypertrophic scar and keloid despite a relative lack of crosslinking in these tissues. In both normal tissues and pathologic scars we have found only normal Type I collagen—based on its chromatographic behavior and amino acid content.

The fibroblasts cultured from these tissues consist of three phenotypically different (S, A, and K) variants whose relative distribution corresponds with the tissue of origin.

A hypothetical model can be constructed which aids in explaining our findings and other recent discoveries concerning the biosynthesis and regulation of scar formation.

The results of these studies lead to the conclusion that hypertrophic scar and keloid are not separate and distinct pathologic entities. They are best characterized as similar aberrations which occupy to a greater or lesser degree the abnormal pole of the spectrum of human wound healing and scar maturation.

References

1. Ketchum LD, Cohen IK, Masters FW: Hypertrophic scars and keloids: A collective review. Plast Reconstr Surg 53:140–154, 1974
2. Ramachandran GN (Editor): Treatise on Collagen, Vol 1. London, Academic Press, Inc., 1967
3. Bornstein P: The biosynthesis of collagen. Annu Rev Biochem 43:567–603, 1974
4. Nimni M: Metabolic pathways and control mechanisms involved in the biosynthesis and turnover of collagen in normal and pathological connective tissues. J Oral Pathol 2:175–202, 1973
5. Gallop PM, Blumenfeld OO, Seifter S: Structure and metabolism of connective tissue proteins. Annu Rev Biochem 41:617–672, 1972

6. Grant ME, Prockop DJ: The biosynthesis of collagen. N Engl J Med 286:242–249, 1972
7. Traub W, Piez KA: The chemistry and structure of collagen. Adv Protein Chem 25:243–352, 1971
8. Hudson BG, Spiro RG: Fractionation of glycoprotein components of the reduced alkylated renal glomerular basement membrane. J Biol Chem 247:4239–4247, 1972
9. Siegel RC, Pinnell SR, Martin GR: Cross-linking of collagen and elastin: Properties of lysyl oxidase. Biochemistry 9:4486–4492, 1970
10. Siegel RC: Biosynthesis of collagen crosslinks: Increased activity of purified lysyl oxidase with reconstituted collagen fibrils. Proc Natl Acad Sci USA 71:4826–4830, 1974
11. Miller EJ: Isolation and characterization of a collagen from chick cartilage containing three identical alpha chains. Biochemistry 10:1652–1659, 1971
12. Trelstad RL, Kang AH, Igarashi S, Gross J: Isolation of two distinct collagens from chick cartilage. Biochemistry 9:4993–4998, 1970
13. Chung E, Miller EJ: Collagen polymorphism: Characterization of molecules with the chain composition [alpha $1(III)_3$] in human tissues. Science 183:1200–1201, 1974
14. Daniels JR, Chu GH: Basement membrane collagen of renal glomerulus. J Biol Chem 250:3531–3537, 1975
15. Kefalides NA: Isolation of collagen from basement membrane containing three identical alpha chains. Biochem Biophys Res Commun 45:226–234, 1971
16. Harris ED Jr, Krane SM: Collagenases. N Engl J Med 291:557–563, 1974
17. Kang AH, Nagai Y, Piez KA, Gross J: Studies on the structures of collagen utilizing a collagenolytic enzyme from tadpole. Biochemistry 5:509–515, 1966
18. Eisen AZ, Jeffrey JJ, Gross J: Human skin collagenase: Isolation and mechanism of attack on the collagen molecule. Biochim Biophys Acta 151:637–645, 1968
19. Lazarus GS, Decker JL, Oliver CH, Daniels JR, Multz CV, Fullmer HM: Collagenolytic activity of synovium in rheumatoid arthritis. N Engl J Med 279:914–919, 1968
20. Finlay JB, Hunter JAA, Steven FS: Preparation of human skin for high resolution scanning electron microscopy using phosphate buffered crude bacterial alpha-amylase. J Microsc (Oxf) 93:73–76, 1971
21. Lewis ER, Nemanic MK: Critical point drying techniques. Scanning Electron Microscopy. Chicago, IIT Research Institute, 1973, pp 767–774
22. Hayflick L, Moorhead PS: The serial cultivation of human diploid cell strains. Exp Cell Res 25:585–621, 1961
23. Merrill JT, Veizades N, Hulett HR, Woulf PL, Herzenberg LA: An improved cell volume analyzer. Rev Sci Instrum 42:1157–1163, 1971
24. Drake MP, Davison PF, Bump S, Schmitt FO: Action of proteolytic enzymes on tropocollagen and insoluble collagen. Biochemistry 5:301–312, 1966
25. Cohen IK, Keiser HR, Sjoerdsma A: Collagen synthesis in human keloid and hypertrophic scar. Surg Forum 22:488–489, 1971
26. Cohen IK, Beaven MA, Horakova Z, Keiser HR: Histamine and collagen synthesis in keloid and hypertrophic scar. Surg Forum 23:509–510, 1972
27. Morgan PH, Jacobs HG, Segrest JP, Cunningham LW: A comparative study of glycopeptides derived from selected vertebrate collagens. J Biol Chem 245:5042–5048, 1970
28. Grant ME, Freeman IL, Schofield JD, Jackson DS: Variations in the carbohydrate content of human and bovine polymeric collagens from various tissues. Biochim Biophys Acta 177:682–685, 1969
29. Spiro RG: Characterization and quantitative determination of the hydroxylysine-linked carbohydrate units of several collagens. J Biol Chem 244:602–612, 1969

30. Deshmukh K, Nimni M: A defect in the intramolecular and intermolecular cross-linking of collagen caused by penicillamine. II. Functional groups involved in the interaction process. J Biol Chem 2244:1787–1795, 1969
31. Bentley JP: The biological role of the ground substance mucopolysaccharides. The Dermis. Edited by W Montagna, JP Bentley, EF Dobson. New York, Appleton-Century-Crofts, 1970, p 103
32. Wood GC: The precipitation of collagen fibers from solution. International Review of Connective Tissue Research, Vol 2. Edited by DA Hall. New York, Academic Press, Inc., 1964, pp 1–31
33. Keech MK: The formation of fibrils from collagen solutions. IV. Effect of mucopolysaccharides and nucleic acids: An electron microscope study. J Biophys Biochem Cytol 9:193–209, 1961
34. Jackson DS, Bentley JP: Collagen-glycosaminoglycan interactions. Treatise on Collagen, Vol 2A. Edited by GN Ramachandran. New York, Academic Press, Inc. 1968, pp 189–214
35. Kischer CW, Shetlar MR: Collagen and mucopolysaccharides in the hypertrophic scar. Connect Tissue Res 2:205–213, 1974
36. Eisen AZ: Human skin collagenase: Localization and distribution in normal skin. J Invest Dermatol 52:442–448, 1969
37. Donoff RB, McLennan JE, Grillo HC: Preparation and properties of collagenases from epithelium and mesenchyme of healing mammalian wounds. Biochim Biophys Acta 227:639–653, 1971
38. Rokosova-Cmuchalova B, Bentley JP: Relation of collagen synthesis to chondroitin sulfate synthesis in cartilage. Biochem Pharmacol (Suppl):315–328, 1968

[*Illustrations follow*]

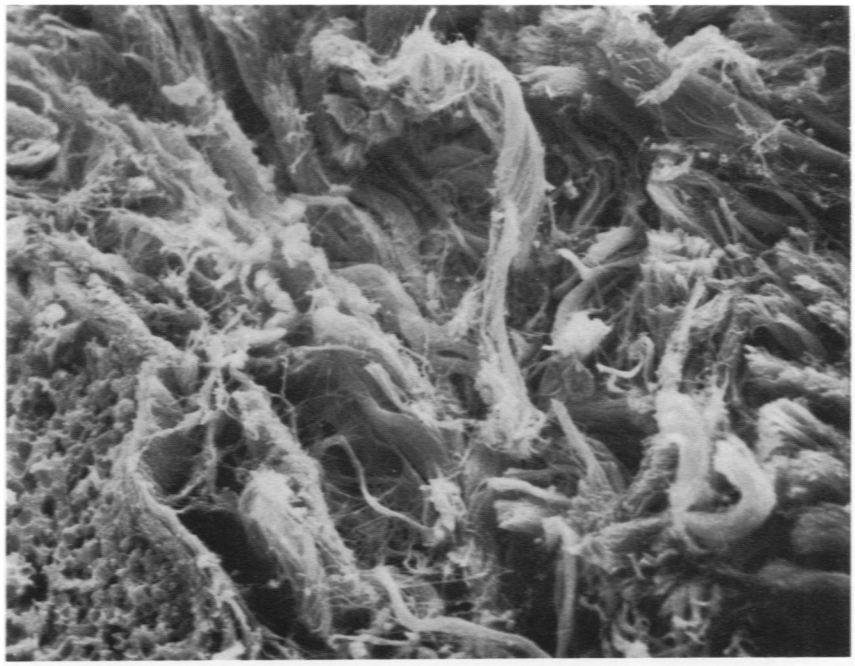

A

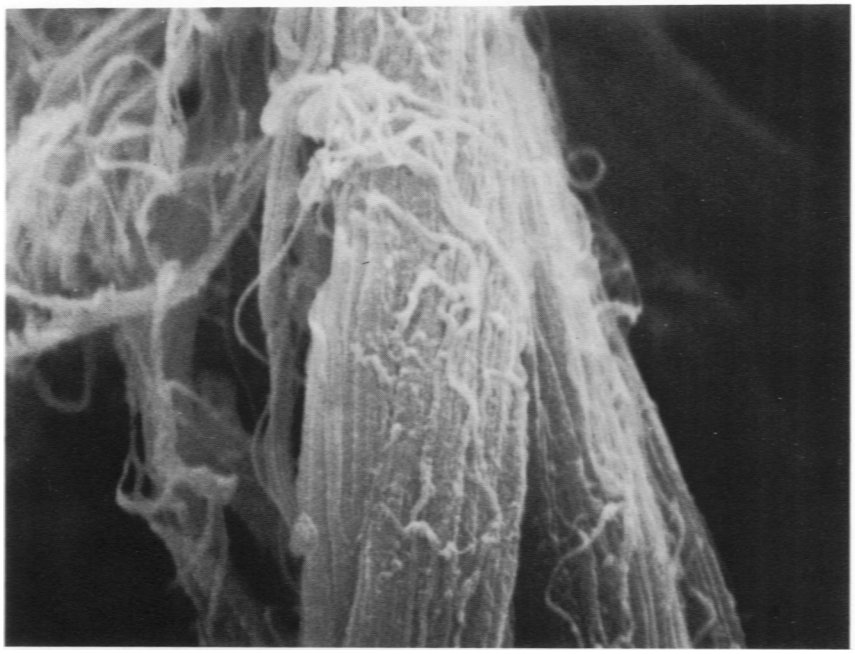

B

Figure 1A—Normal dermal collagen bundles. Basement membrane and epithelial layer are seen in the *left lower corner* of the micrograph. Fine interconnecting fibers lie among the collagen bundles. (× 500) **B**—Normal dermal collagen bundle. Compactly arrayed parallel fibers comprise bundles 8 to 10 μ in diameter. (× 5000)

A

B

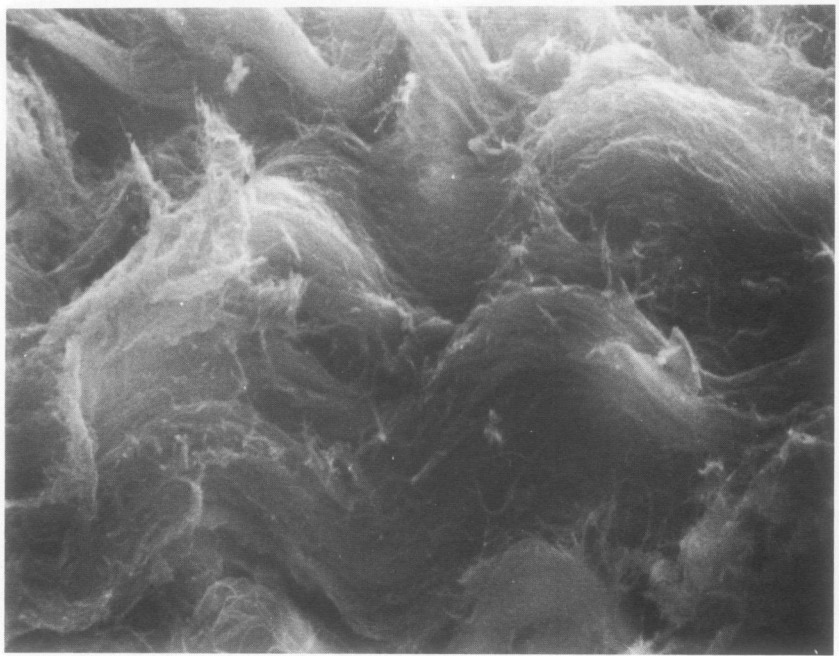

Figure 2A—Hypertrophic scar collagen. Bundle formation is less ordered and interrelationships more random than in normal skin or mature scar. (× 500) **B**—Hypertrophic scar collagen. Fibers are loosely arrayed in a wavy pattern. Individual fibers often appear attenuated. (× 2000)

A

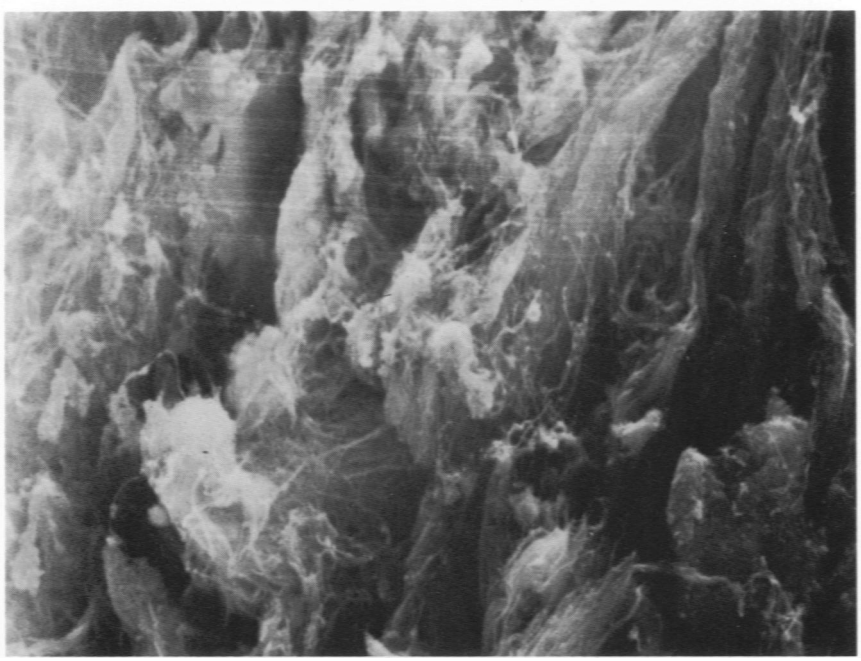

B

Figure 3A—Keloid collagen. Discrete bundle formation is lacking. Collagen is arranged in randomly oriented loose sheets. (× 500) **B**—Keloid collagen. Fibers fail to form bundles and are arrayed in loose, wandering, random fashion. (× 2000)

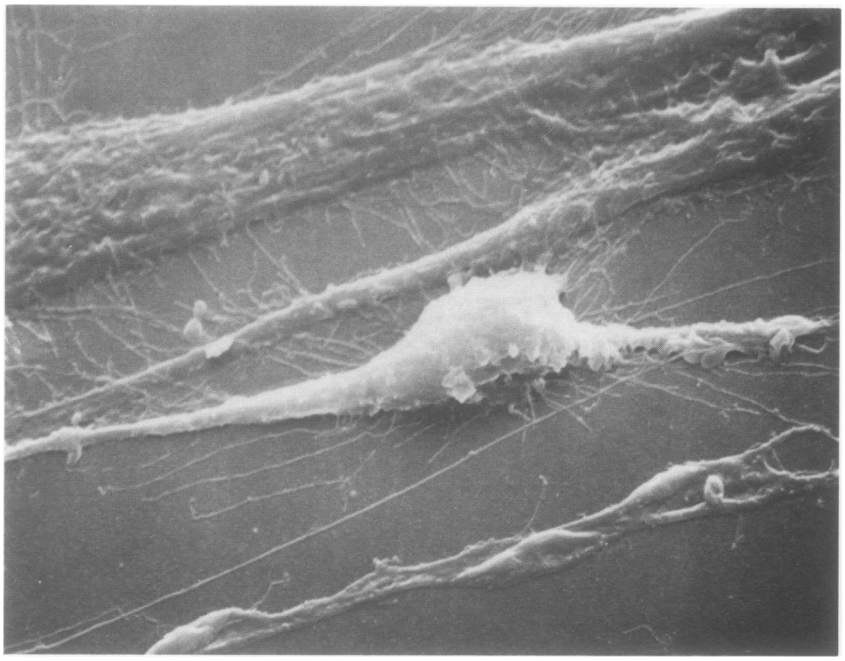

Figure 4—S type fibroblast. Note the rough cytoplasmic surface and bipolar spindle shape. (× 2000)

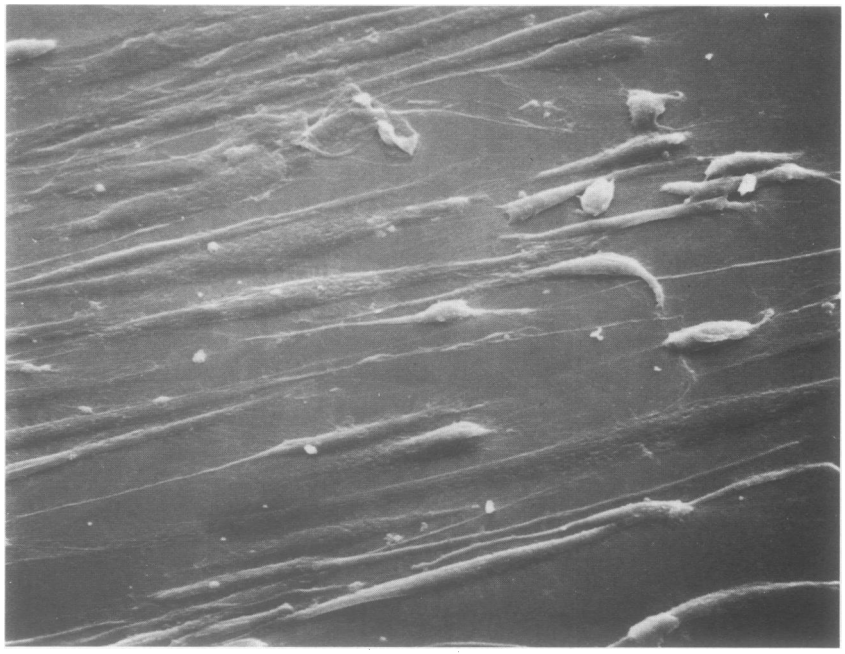

Figure 5—Hypertrophic scar-derived fibroblasts. Many of both S and A type cells are scattered throughout the field. (× 400)

Figure 6—Keloid-derived fibroblasts. The K type cell is noted as a separate entity. (× 500)

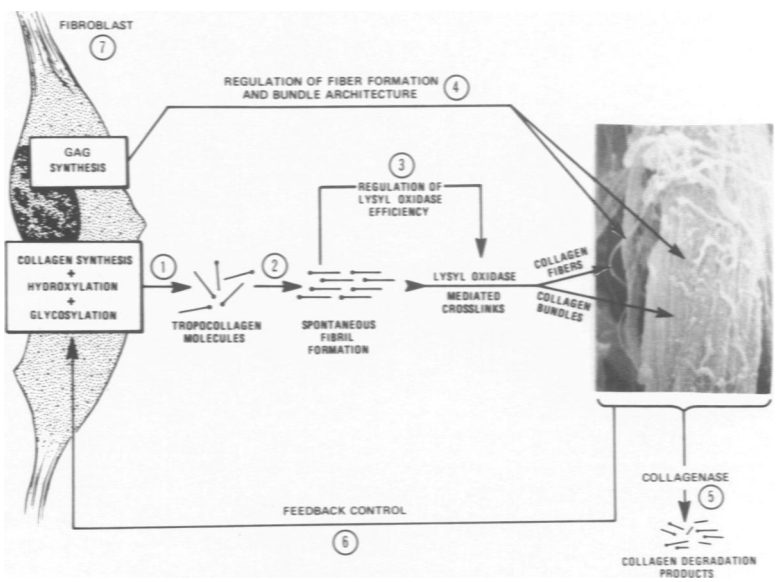

Figure 7—Regulation of collagen biosynthesis and morphogenesis—a hypothetical model.

[*End of Article*]